Electronic Supplementary Material (ESI) for Catalysis Science & Technology.

Chemistry of iron and copper co-doped zinc oxide: reduction and degradation of pollutants

Hiwot Belay,[a] Buzuayehu Abebe,*[a] Dereje Tsegaye,*[a] C R Ravikumar,[b] S. Giridhar Reddy,[c] and H C Ananda Murthy *†[a]

[a.] *Adama Science and Technology University, Department of Applied Chemistry, 1888, Adama, Ethiopia.*
[b.] *East-West Institute of Technology, Department of Science, Bangalore, 560091, India.*
[c.] *Amrita Vishwa Vidyapeetham, Determent of Chemistry, Bengaluru, 560035, India*
†Saveetha University, Department of Prosthodontics, Chennai, 600077, Tamil Nadu, India

Characterizations

The material's thermal stability was determined by thermogravimetric-differential thermal analysis (TGA-DTA; S/N: C30575100456TK; detector: DTG-60H) in a nitrogen atmosphere with a flow rate of 50 mL/min. The crystallinity, doping, and heterojunction analysis was conducted by X-ray diffraction technique (XRD, Shimadzu-7000, at a radiation wavelength of 0.15406 nm, voltage of 40 kV, and current of 30 mA). The material's morphology, composition, and elemental mapping were analyzed by field emission scanning electron microscopes (FE-SEM, ZEISS SIGMA VP). The optical and electron-hole recombination properties before and after doping were studied by photoluminescence spectroscopy (PL, CaryEclipse fluorescence spectrophotometer S/N: MY18490002, the scan rate being 600 nm/min) with a laser excitation wavelength of 325 nm. Chemical bonding and stiffness before and after calcination by FT/IR-6600typeA (S/N: A013861790), 2 mm/sec scanning speed, detector TGS. Further material's optical properties and energy band gap were assessed by a double beam ultraviolet-visible (UV-vis, P9 spectrophotometer).

Figures

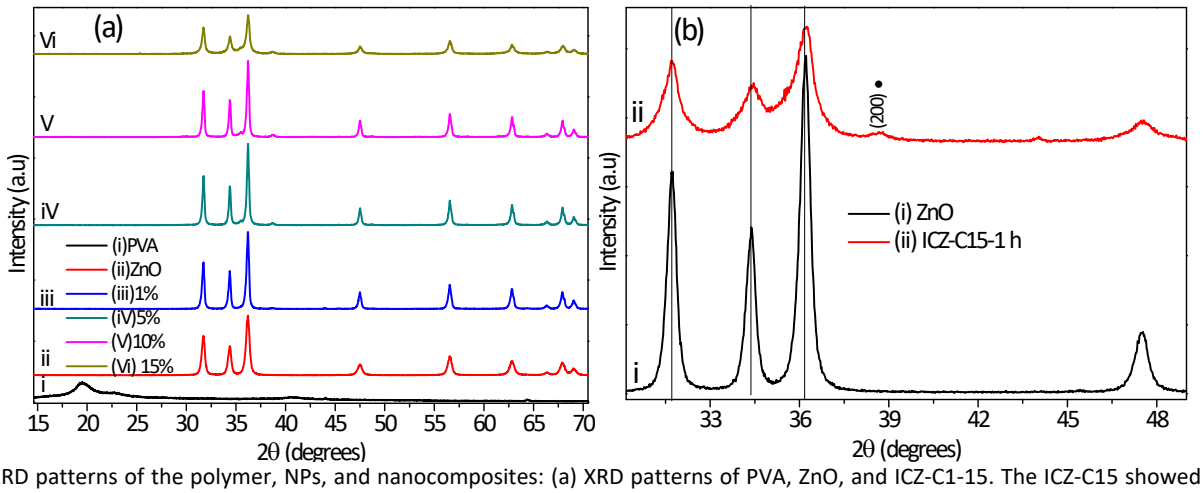

Fig. S1 XRD patterns of the polymer, NPs, and nanocomposites: (a) XRD patterns of PVA, ZnO, and ICZ-C1-15. The ICZ-C15 showed greater surface area as compared to the others. (b) The magnified XRD patterns of ZnO and ICZ-C15. Only the CuO phase was detected on the XRD patterns of the composite. Slight high angle shift for the composites were observed compared to ZnO NPs

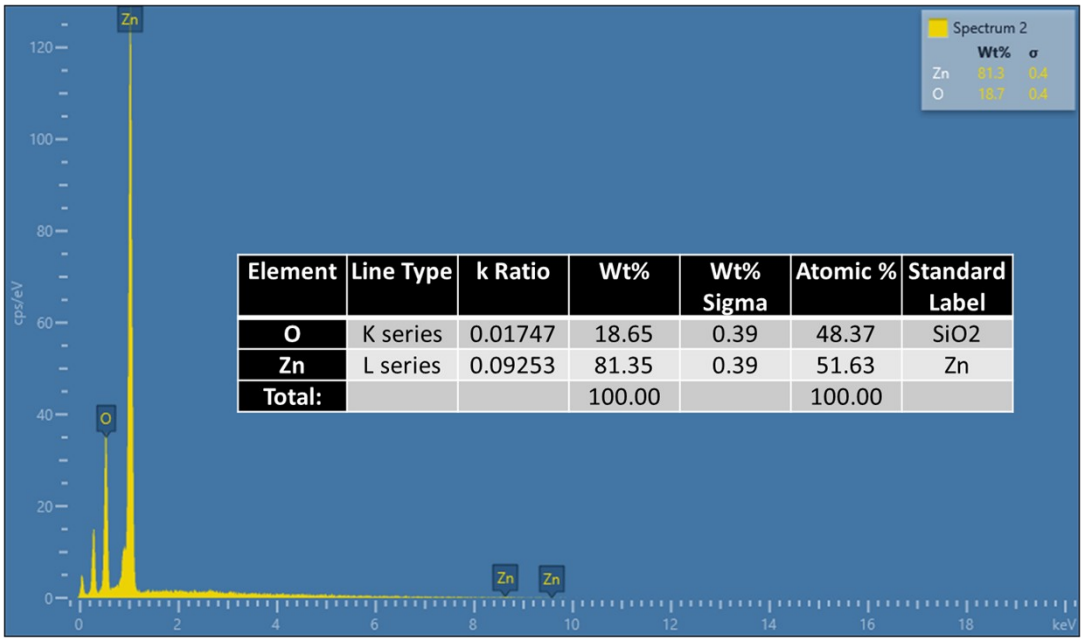

Element	Line Type	k Ratio	Wt%	Wt% Sigma	Atomic %	Standard Label
O	K series	0.01747	18.65	0.39	48.37	SiO2
Zn	L series	0.09253	81.35	0.39	51.63	Zn
Total:			100.00		100.00	

Fig. S2 EDX compositional analysis spectra for ZnO NPs: The EDX analyses show the presence of only zinc and oxygen, without impurities. The inset table in the EDX spectra shows the composition of the elements.

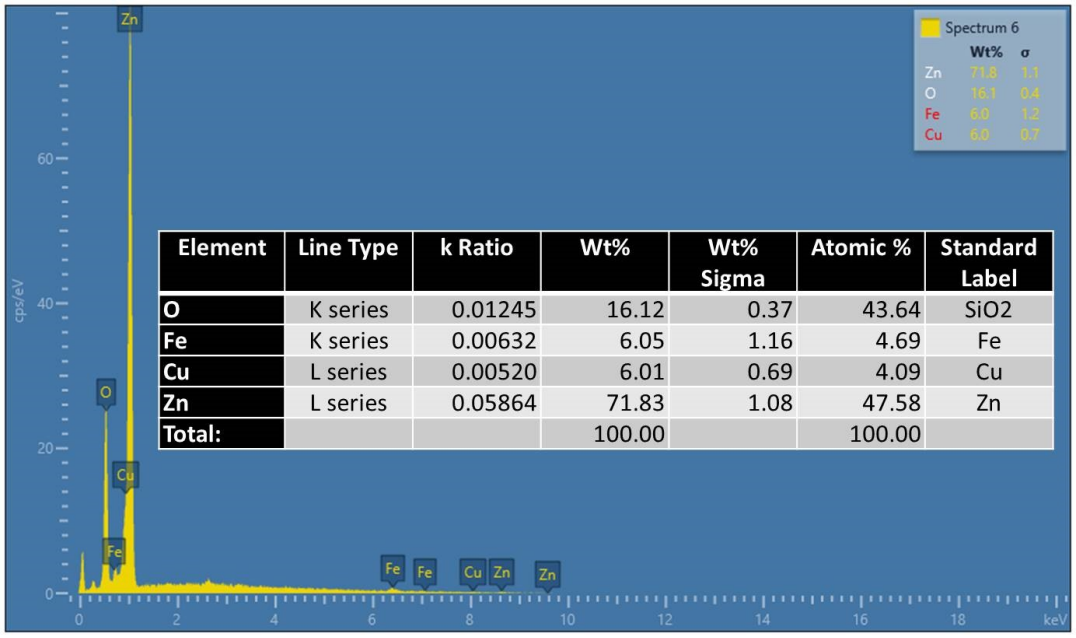

Element	Line Type	k Ratio	Wt%	Wt% Sigma	Atomic %	Standard Label
O	K series	0.01245	16.12	0.37	43.64	SiO2
Fe	K series	0.00632	6.05	1.16	4.69	Fe
Cu	L series	0.00520	6.01	0.69	4.09	Cu
Zn	L series	0.05864	71.83	1.08	47.58	Zn
Total:			100.00		100.00	

Fig. S3 The EDX compositional analysis spectra for ICZ-C show the presence of zinc, iron, copper, and oxygen without any other impurities. The inset table in the EDX spectra shows the composition of the elements in the perfect proportion for iron and copper, also in accordance with the precursor's amount taken during synthesis.

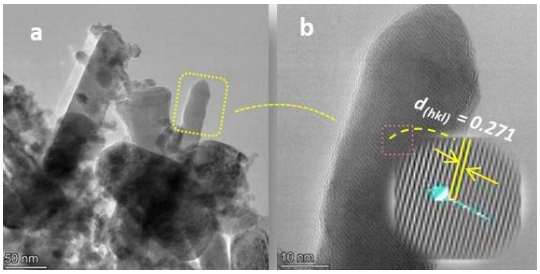

Fig. S4 ICZ-C15 morphology and crystallinity investigation using TEM/HRTEM techniques; (a) TEM and (b) HRETM images of ICZ-C15.

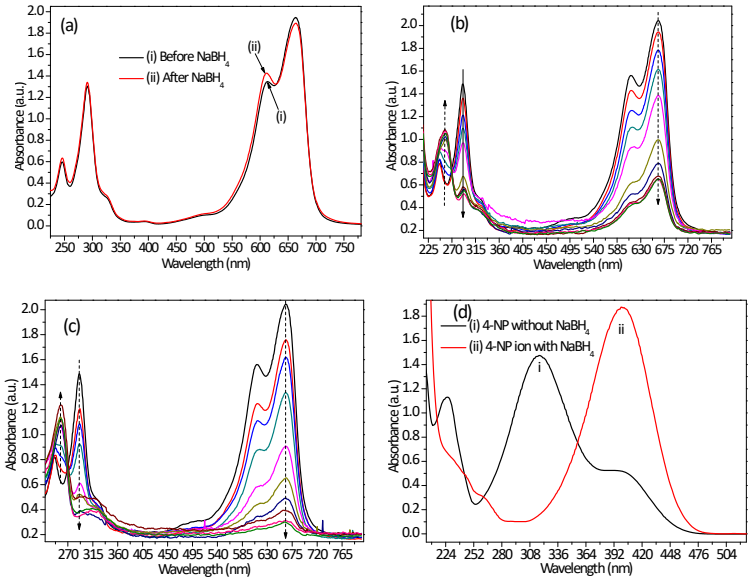

Fig. S5 Catalytic reduction reaction for NPs and NCs in the presence and absence of $NaBH_4$: (a) the methylene blue spectrum in the presence and absence of $NaBH_4$; (b and c) the reduction result in the presence of $NaBH_4$ and 1 and 10% ICZ-Cs, respectively; (d) the 4-nitrophenol spectrum in the absence and presence of $NaBH_4$.

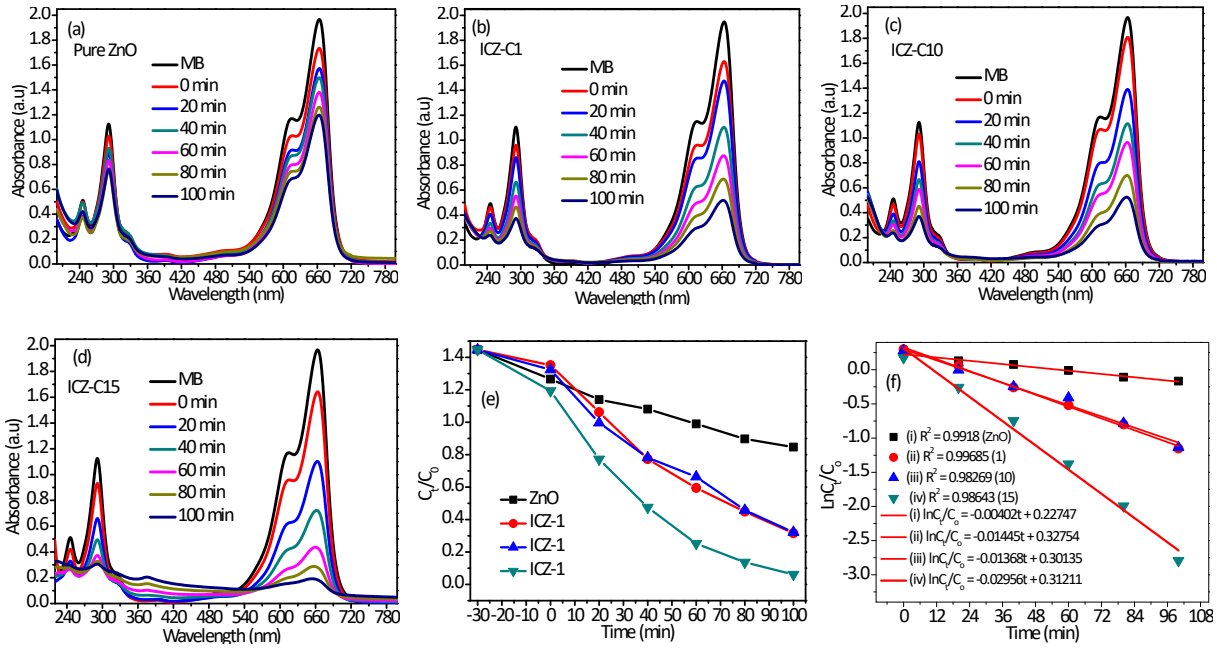

Fig. S6 Effect of precursor percentage optimization on methylene blue dye degradation: photocatalytic activity of (a) ZnO, (b) ICZ-C1, (c) ICZ-C10, and (d) ICZ-C15. (e and f) are C_t/C_o versus time and $\ln C_t/C_o$ versus time plots of ZnO NPs and ICZ-Cs with 1, 10, and 15 mg/L concentrations, respectively, at a solution pH of 6.5 and a methylene blue dye concentration of 10 mg/L.

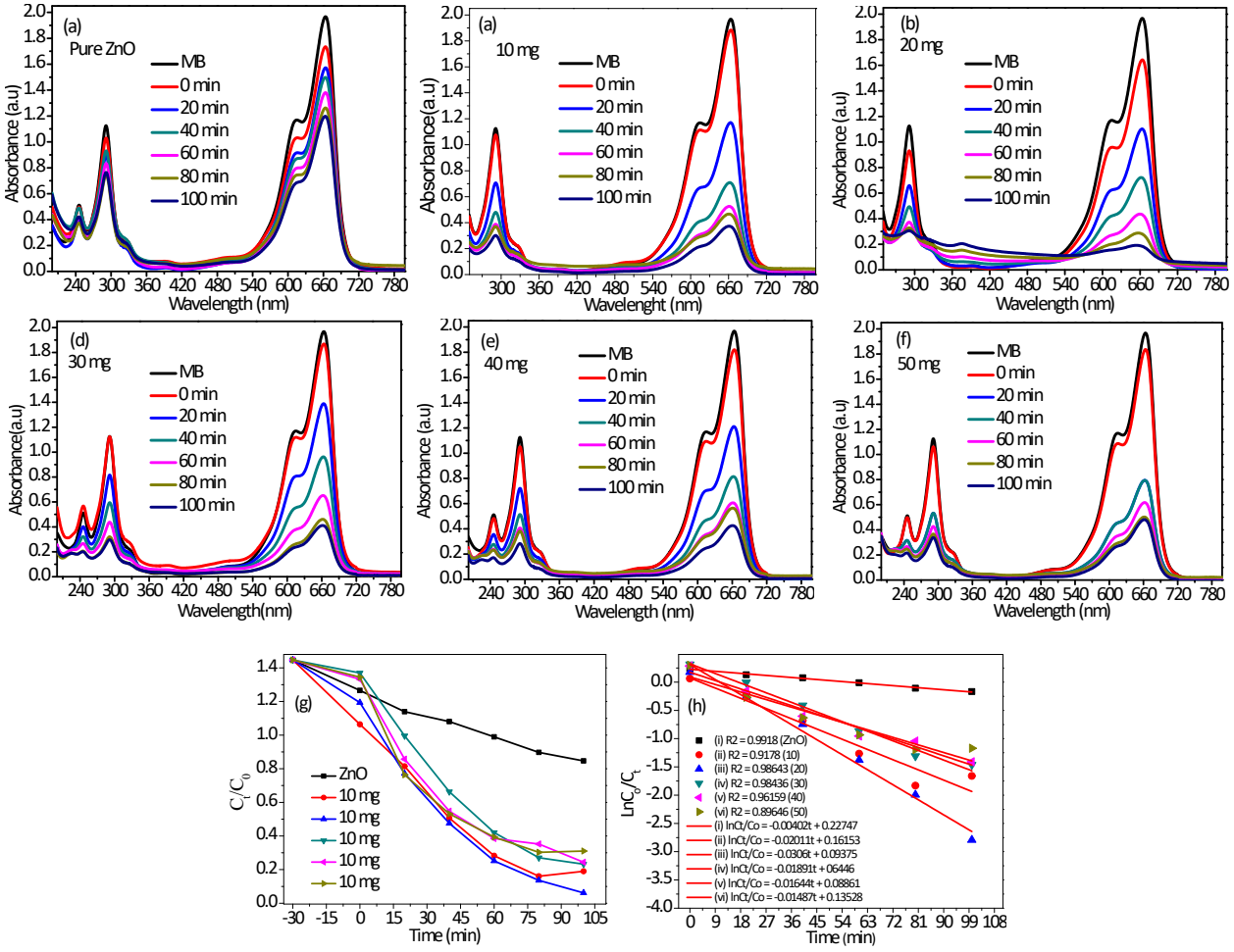

Fig. S7 Effect of catalyst dosage on methylene blue dye degradation: photocatalytic activity of (a) ZnO NPs and ICZ-C15 with (b) 10 mg, (c) 20 mg, (d) 30 mg, (e) 40 mg, and (f) 50 mg. (g and h) are C_t/C_o versus time and $\ln C_t/C_o$ versus time plots of ZnO NPs and ICZ-Cs with 10, 20, 30, 40, and 50 mg amounts, respectively, at a solution pH of 6.5 and a methylene blue dye concentration of 10 mg/L.

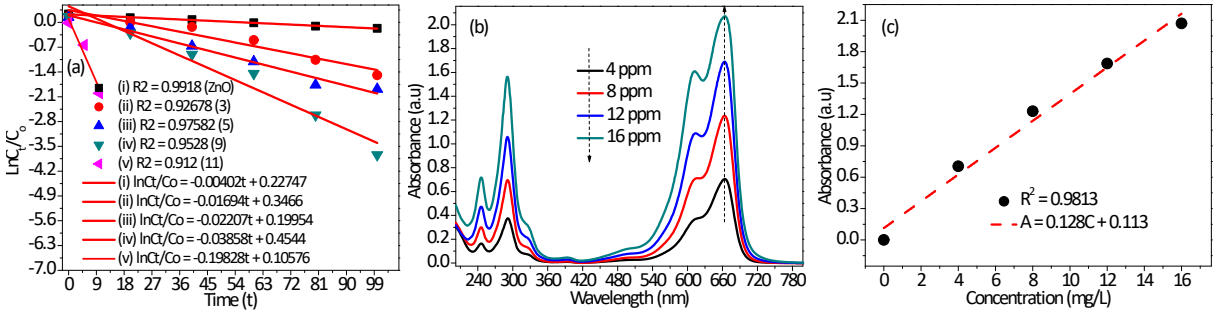

Fig. S8 $\ln C_t/C_o$ versus time plot of ZnO NPs and ICZ-Cs with solution pH of 3, 5, 9, and 11 at a catalyst dosage of 20 mg and a methylene blue dye concentration of 10 mg/L. (b) Absorbance versus wavelength spectrum plots of standard methylene blue dye concentrations ranging from 0 to 16 ppm; (c) absorbance versus concentration calibration curve obtained from Fig. S8b